



## Reconstructing changes in nitrogen input to the Danube-influenced Black Sea Shelf during the Holocene

Andreas Neumann<sup>1</sup>, Justus E.E van Beusekom<sup>1</sup>, Alexander Bratek<sup>1,2</sup>, Jana Friedrich<sup>1,4</sup>, Jürgen Möbius<sup>2</sup>,  
Tina Sanders<sup>1</sup>, Hendrik Wolschke<sup>3</sup>, Kirstin Dähnke<sup>1</sup>

5 1 Helmholtz-Zentrum Hereon, Institute of Carbon Cycles, Geesthacht, Germany

2 Universität Hamburg, Center for Earth System Research and Sustainability, Institute of Geology, Hamburg, Germany

3 Helmholtz-Zentrum Hereon, Institute of Coastal Environmental Chemistry, Geesthacht, Germany

4 IAEA Marine Environment Laboratories, Department of Nuclear Sciences and Applications, International Atomic Energy Agency, 98000 Monaco, Principality of Monaco

*Correspondence to:* Andreas Neumann (andreas.neumann@hereon.de)

10 **Abstract.** The western Black Sea shelf, where Danube River contributes the largest river discharge into the Black Sea, is particularly sensitive to river-induced eutrophication, which peaked in the 1980s and 1990s due to human-induced nutrient input. Nutrient input to the western Black Sea shelf and eutrophication is decreasing since the mid-1990s due to the collapse of eastern European economies after 1989 and ongoing mitigation measures to reduce nutrient emissions. The assessment of nutrient inputs to the Black Sea prior to the 1960s however is complicated by the scarcity of information on earlier Danube  
15 nutrient loads. Thus, to define what pristine conditions have looked like to provide a reference for nutrient reduction targets remains challenging. In this study, we aim to trace modern and historical nitrogen sources to the western Black Sea Shelf during the last ~5,000 years with special focus on the past 100 years, using sedimentary records of TOC, TIC, nitrogen, and  $\delta^{15}\text{N}$ .

20 Our results demonstrate that the balance of riverine nitrogen discharge into the Black Sea on the one hand, and nitrogen fixation in the pelagic system on the other, seem largely determined by climate effects. Specifically, this balance of riverine N input and N fixation is not only controlled by the concentration of nutrients discharged by rivers, but also by the freshwater volume, which controls the intensity of thermohaline stratification and thereby the timing and intensity of nutrient recycling from the deep basin back into the euphotic epipelagic. Based on analytical data of geochemical and isotopic properties of dated sediment  
25 cores, we identified a gradient from the nearshore sediment directly at the Danube Delta, where riverine N is dominant to offshore sediment in 80 m water depth, with pelagic N fixation being dominant in the past. Our results based on stable isotopes also demonstrate the increased deposition of nitrogen from human activities in all stations across the shelf and the concomitant changes in deposition rates of organic matter as indication for perturbations in the epipelagic community due to the human-induced eutrophication. Finally, our stable isotope data indicate that human-induced eutrophication can be traced back to the  
30 12<sup>th</sup> century CE, which raises the question which point in time is a feasible reference for nutrient reduction goals as the Danube nutrient loads was not pristine since at least in the 800 years.



## 1 Introduction

The Black Sea is a semi-enclosed sea, which is connected to the Mediterranean through the Bosphorus. The limited inflow of saline Mediterranean water through the Bosphorus in combination with freshwater discharge by the rivers creates strong 35 thermohaline stratification, which separates the ventilated surface water from oxygen-free, euxinic waters, creating the largest anoxic water body on earth, and hence makes the Black Sea unique. This thermohaline stratification makes the Black Sea very susceptible to climate but also human pressures. The climatic variability in the Black Sea between cold and dry and mild and wet winters and appears to be governed by the North Atlantic Oscillation (NAO) and East Atlantic-West Russia (EAWR) teleconnection patterns (Oguz et al. 2006). The Black Sea exhibits a very efficient coupling between the anthropogenic and 40 climatic forcing, as displayed in driving the dramatic ecosystem changes observed during the 1980s and 1990s (Oguz et al. 2006).

The general circulation of the Black Sea is dominated by the persistent Rim Current, which circulates counterclockwise along the shelf break and horizontally mixes water masses throughout the whole basin (Oguz et al. 2005). Several coastal eddies are 45 part of the Rim Current System and provide additional mixing across the shelf.

The north-western shelf is wider than elsewhere in the Black Sea and is substantially influenced by the discharge of several rivers (Dnipro, Dniester) of which Danube is the most significant. These rivers transport sediments into the coastal zone and the Danube built up a large Delta that spreads out into the Black Sea (Panin et al. 2016, Constantinescu et al. 2023). 50 Additionally, Danube is the largest source of freshwater to the Black Sea, and the discharge intensity directly affects the salinity gradient in the surface water particularly in the western the Black Sea and thereby the intensity of stratification. The degree of stratification controls the vertical mixing and thus the ventilation of the deep water with oxygen and also the replenishment of N and P in the euphotic zone at the surface, which determines the susceptibility of Black Sea biogeochemical cycles to climate forcing. A high discharge of freshwater due to Atlantic climate intensifies the stratification and results in an upward shift of 55 the oxycline and a reduced availability of nutrients in the surface water of the central Black Sea and higher availability of riverine nutrients in the river plume (Fulton et al. 2012). Conversely, low discharge of freshwater in boreal climate results in a deep oxycline and the upwelling of deep water that is enriched in phosphorous and depleted in nitrogen (Fulton et al. 2012). Upwelling of low N and high P deep water into the surface water reduces the molar N : P ratio, which favours N-fixation (diazotrophy) and thereby reduces the contribution of riverine N in fuelling primary production (Fuchsman et al. 2008).

60

The Danube River represents the second-largest river in Europe and hence drains a vast catchment area, which has been intensively used by humans since several millennia and thereby turned that river into a significant source of nutrients to the north-western shelf. The increase in European population with spread of agricultural activities peaking first around 250 yr AD, resulted in significant deforestation in central Europe and growth of river deltas (Maselli & Trincardi 2023, Kaplan et al 2009).



65 That sediment transported towards the sea lead to increased nutrient transport and hence, pre-industrial eutrophication. The recent eutrophication of Danube accelerated in the 1960 – 1990 CE period, during the ‘green revolution’), which resulted in a significant eutrophication of the north-western Shelf and a degradation of habitats there (Kovacs & Zavadsky, 2021). Remediation measurements since the early 1990s CE led to a substantial decrease of the Danube DIN load, which is now below the level of 1960 (Kovacs & Zavadsky, 2021). Consequently, Möbius and Dähnke (2015) investigated present-day

70 nutrient inputs to the shelf and argued that the majority of riverine DIN is now taken up in the river plume and that the nitrogen load is exported to the shelf as organic matter.

In this paper, we use nitrogen isotopes to identify nitrogen sources. Analysis of stable isotopes is a versatile tool as they have distinct isotopic signatures, which are expressed using the delta notation in the following. For a start, nitrogen in ammonium

75 and nitrate from fixation of atmospheric N<sub>2</sub> is isotopically light with  $\delta^{15}\text{N}$  values around 0 ‰. This signature is preserved in organisms such as algae, which assimilate dissolved DIN to produce organic nitrogen compounds. However, molecules with the lighter <sup>14</sup>N tend to diffuse and react slightly faster than molecules with the heavier <sup>15</sup>N, which results in kinetic fractionation and slightly increases the relative concentration of <sup>14</sup>N in the product while <sup>15</sup>N is enriched in the remaining substrate. Consequently, the initial isotope signature evolves as the nitrogen is propagating through different pools. The fractionation

80 effects of serial turnover accumulate and cause that ammonium in soils is isotopically enriched to  $\delta^{15}\text{N}$  values in the range of 5 to 10 ‰, while nitrogen in manure and sewage can be isotopically enriched up to 30 ‰. Since the isotopic signature of a nitrogen pool reflects the combined effects of its history such as sources, turnover, and mixing, conclusions about the environment can be drawn from isotopic analyses. Johannsen et al. (2008) and Bratek et al. (2020) demonstrated that the  $\delta^{15}\text{N}$  value of riverine nitrate is closely related to the intensity of anthropogenic land use. Dähnke et al. (2008b) and Serna et al.

85 (2010) used the <sup>15</sup>N signature of anthropogenic nitrogen to identify the onset of human-induced eutrophication of River Elbe in sediment of North Sea and Skagerrak. Similarly, Anderson and Cabana et al. (2006) demonstrated that the  $\delta^{15}\text{N}$  value of riverine nitrate is also related to the DIN load. We will apply this method to plankton biomass that was deposited to the sediment from the Danube-influenced shelf to reconstruct nitrogen sources to this part of the Black Sea.

90 We aimed to reconstruct present and historic nitrogen sources to the Danube-influenced north-western shelf of the Black Sea by analysing sediment cores along a transect from the Danube Delta towards the shelf break. The sediment along this transect reflects the gradient from a dominant influence of the Danube River Plume to the dominant influence of water masses from the open Black Sea, which imprint the specific signature of their respective nitrogen sources into the sediment record. We have analysed the sediment for contents of organic carbon and nitrogen, and the composition of stable nitrogen isotopes to identify

95 natural and anthropogenic nitrogen sources over the past 5000 years.

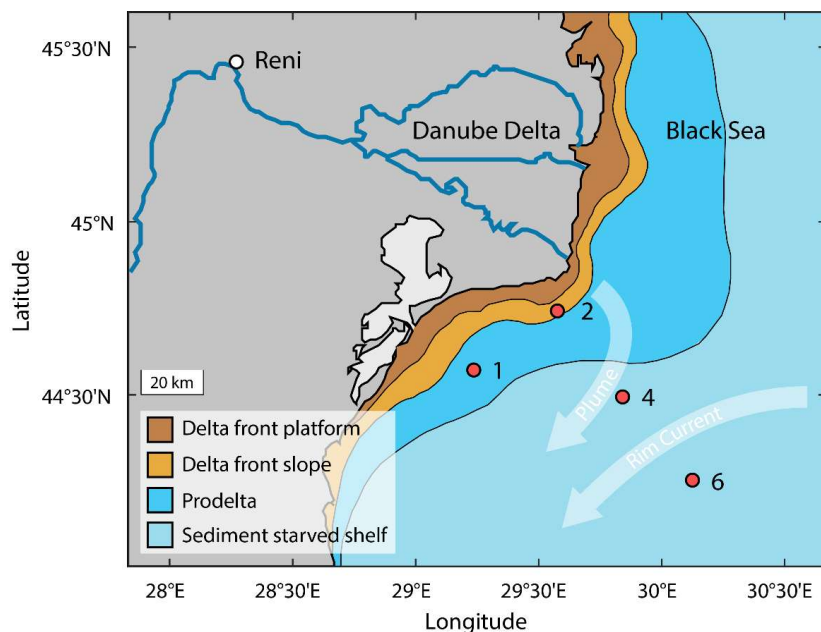


## 2 Material & Methods

### 2.1 Working area and samples

Sampling was performed in early May 2016 during R/V Mare Nigrum cruise MN 148 in the Romanian Shelf area at four stations that span a transect from nearshore to offshore (Tab. 1, Fig. 1). The water depth at the sampling stations ranged from

100 22 m (Station 2) to 80 m (Station 6). From each station, sediment cores (20-40 cm length, 6 cm in diameter) were taken with a Multicorer. The sediment cores were immediately sliced in 1 cm intervals and frozen for further analysis. The sediment from stations 4 and 6 was wet sieved through a 400  $\mu\text{m}$  sieve after slicing to collect mussel shells for radiocarbon dating. The <400  $\mu\text{m}$  fraction was freeze-dried and homogenized for analysis of  $\delta^{15}\text{N}$ , organic carbon and nitrogen content.



105

**Figure 1:** Map showing the sampling stations of the sediment cores 1, 2, 4 and 6 in the northwestern Black Sea during RV Mare Nigrum cruise 148 and major depositional units of the Danube Delta (after Panin et al. 2016). The light arrows indicate the general surface water currents of Danube River Plume and Rim Current.

110



Table 1: Summary of meta data of sediment cores from Mare Nigrum cruise 148.

Core	Latitude	Longitude	Water depth (m)	Core length (m)
1	45° 58.4	29° 18.8°	30	42
2	44° 74.9	29° 58.2°	27	35
4	44° 49.9	29° 84.8°	62	29
6	44° 25.2	30° 13.1°	80	27

## 2.2 Analyses of sediment samples

115 The sediment samples were analysed for total carbon and total nitrogen content with an elemental analyser (Carlo Erba NA 1500) via gas chromatography, calibrated against acetanilide. The total organic carbon content (TOC) was analysed after a threefold removal of inorganic carbon using 1 mol L<sup>-1</sup> hydrochloric acid. Sediment carbonate content was then calculated as the difference of total carbon content and TOC content. The standard deviation of sediment samples was better than 0.6% for TOC and 0.08 % for nitrogen.

120 Nitrogen isotope analyses were performed with a CE 1108 elemental analyser (Thermofinnigan) connected to a mass spectrometer (Finnigan 252) via a split interface (Conflow). Two international standards were used for calibration (IAEA-N1: δ<sup>15</sup>N = 0.4 ‰, IAEA-N2: δ<sup>15</sup>N = 20.3 ‰), and an additional, internal standard was measured for further quality assurance. The standard deviation for repeated measurements was < 0.2 ‰.

## 2.3 Radiocarbon Dating

125 The radiocarbon ages of organic sediment (TOC) were obtained from 2 bulk sediment samples from Station 4, and 6 bulk sediment slices from Station 6. Additionally, 6 bivalve shells from different sediment layers of Station 6 (two samples of *Modiolula phaseolina* and four samples of *Mytilus galloprovincialis*) were analysed to date the carbonate. These two species were used because the top 8 cm of the sediment are characterized by *Modiolula phaseolina*, whereas *Mytilus galloprovincialis* is dominant in deeper layers. The radiocarbon analyses were carried out at Beta Analytic Inc., U.K., following standard procedures for accelerator mass spectrometry (AMS) radiocarbon dating. The radiocarbon ages are corrected for δ<sup>13</sup>C. Calibration of the radiocarbon ages to years BP (0 a BP = 1950 CE) is according to the age calibration of Stuiver et al. 1998. The sample ages were further corrected with a reservoir age of 500 ± 40 years (Siani et al. 2000). The age of sediment samples between dated samples was estimated by linear interpolation.



## 2.4 Radiometric measurements

135 For  $^{137}\text{Cs}$ ,  $^{226}\text{Ra}$ , and  $^{210}\text{Pb}$  measurement low-level gamma spectrometry was used. Sample preparation was carried out as described in Bunzel et al. (2020). Briefly, the cores were sectioned into slices of 1 cm thickness and frozen during transportation and storage. Each section was dried, and homogenized by a ball mill. Aliquots of each sample were sealed in gas-tight Petri dishes and stored for minimum 28 days for equilibration of Radium-226 with daughter isotopes  $^{222}\text{Rn}$ ,  $^{214}\text{Pb}$  and  $^{214}\text{Bi}$ . Measurements were performed by a High-purity low-level germanium detector (BE 3830P-7500SL-ULB Mirion Technologies  
140 / Canberra, Ruesselsheim, Germany). Measurement times varied between 90 000 s - 600 000 s depending on sample activity. For calibration an artificial reference material was prepared from silica gel and reference solutions of  $^{137}\text{Cs}$  and  $^{226}\text{Ra}$ . (Eckert & Ziegler Nuclitec GmbH, Braunschweig, Germany).

## 2.5 Data integration

145 Sediment ages of cores 1 and 2 are based on results of Constantinescu et al. (2023), which sampled the same stations simultaneously and applied  $^{210}\text{Pb}$  and  $^{137}\text{Cs}$  dating. Observed Danube DIN loads are based on data from Kovacs & Zavadsky (2021), which presented DIN loads at Reni station at the upstream margin of the Danube Delta (Fig. 1). Both datasets were mapped to the corresponding sediment depths of cores 1 and 2 by linear interpolation. As the result, an interpolated  $^{210}\text{Pb}$  /  $^{137}\text{Cs}$  age and an interpolated DIN load was assigned to each of our sediment measurements of cores 1 and 2.

150



### 3 Results

#### 3.1 Radioisotope measurements and dating

Sediment organic matter at Station 4 was dated  $1030 \pm 50$  years at 7.5 cm core depth and  $2580 \pm 50$  years at 16.5 cm core depth by radiocarbon ( $^{14}\text{C}$ ) dating. The age of organic sediment at Station 6 spans from  $60 \pm 50$  years at the sediment surface

155 to  $4880 \pm 50$  years at 16.5 cm depth. Radiocarbon-based ages of bivalve shell carbonates at Station 6 span from  $3130 \pm 50$  years at the sediment surface to  $5070 \pm 50$  years at 16.5 cm depth. The results of radiocarbon dating are summarised in Table 2 and plotted in Figure 2. At Station 6, dated carbonates were systematically older than the organic sediment, and this difference was larger at the sediment surface than at depths (Tab. 2, Fig. 2). No radiocarbon measurements were performed on sediment of Station 1 and 2.

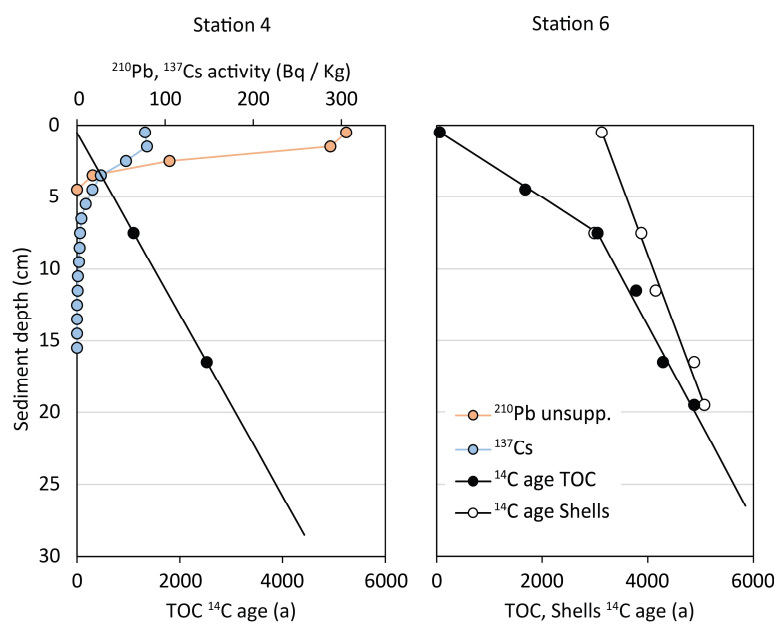
160

Additionally,  $^{137}\text{Cs}$  and unsupported  $^{210}\text{Pb}$  were measured in Station 4 sediment, where unsupported  $^{210}\text{Pb}$  was highest at the sediment surface (306 Bq / kg dry sed.) and decreased exponentially with depth.  $^{210}\text{Pb}$  was below detection limit below 4 cm sediment depth (Fig. 2). Similarly,  $^{137}\text{Cs}$  activity was highest at the sediment subsurface (79 Bq / kg dry sed.), but was detectable to deeper sediment layers than unsupported  $^{210}\text{Pb}$  (Fig. 2). No  $^{210}\text{Pb}$  and  $^{137}\text{Cs}$  measurements of sediment from

165 Station 6 is available.

Table 2: Results of radiocarbon dating of bulk sediment and carbonate shells from Cores 4 and 6. The uncertainty of conventional  $^{14}\text{C}$  dates was generally  $\pm 30$  a, and for calibrated calendar years  $\pm 50$  a, respectively. 0 a BP equals 1950 CE.

Core	Sediment depth (cm)	Material	Conventional $^{14}\text{C}$ age (a)	Calibrated calendar years (a BP)
4	7.5	organic sediment	1530	1030
4	16.5	organic sediment	3080	2580
6	0.5	organic sediment	560	60
6	4.5	organic sediment	2180	1680
6	7.5	organic sediment	3550	3050
6	11.5	organic sediment	4280	3780
6	16.5	organic sediment	4790	4290
6	19.5	organic sediment	5380	4880
6	0.5	carbonate ( <i>Modiolula phaseolina</i> )	3630	3130
6	7.5	carbonate ( <i>Modiolula phaseolina</i> )	3490	2990
6	7.5	carbonate ( <i>Mytilus galloprovincialis</i> )	4380	3880
6	11.5	carbonate ( <i>Mytilus galloprovincialis</i> )	4650	4150
6	16.5	carbonate ( <i>Mytilus galloprovincialis</i> )	5380	4880
6	19.5	carbonate ( <i>Mytilus galloprovincialis</i> )	5570	5070



170

**Figure 2: Results of radioisotope analyses of Cores 4 and 6: Radiocarbon ( $^{14}\text{C}$ ) ages of organic sediment (black circles), radiocarbon ages of carbonate shells (white circles). Measurements of unsupported  $^{210}\text{Pb}$  (orange circles) and  $^{137}\text{Cs}$  (blue circles).**

### 3.2 Sediment cores

175 The characteristics of sampled sediment reflected the proximity of the respective stations to the shore and the Danube Delta. Station 1 was in the shallow Prodelta (Fig. 1), where the sediment was layered mud with various shades of grey, and black layers at 28 cm, 37 cm, 41 cm, and 44 cm sediment depth. Living *Mytilus* bivalves were found at the top layer and empty *Mytilus* shells within the black layers. Core 2 was sampled from the delta front slope (Fig. 1), and sediment was layered mud with various shades of beige, grey, and black. Stations 4 and 6 were in the sediment staved shelf (Fig. 1) where sedimentation rates were lowest. In Core 4, the top 0-3.5 cm were *Modiolula* shells in grey mud, then grey mud without shells down to 6 cm, and light grey mud from 6 to 26 cm sediment depth. Similarly in Core 6, *Modiolula* shells in mud were found at the top 0-5 cm, followed by light grey mud in 5-10 cm, and grey mud in 10-15 cm sediment depth. In 15-20 cm sediment depth, we found dark grey mud, and black mud with *Mytilus* shells in 20-25 cm depth.

180

185 Generally, N stable isotopic composition of sediment ( $\delta^{15}\text{N}$ ) follows a gradient from the shore towards to open Black Sea: The entire nearshore sediment cores of stations 1 and 2 are isotopically enriched (mean  $\delta^{15}\text{N} = 6.7 \text{ ‰}$ ) with respect to

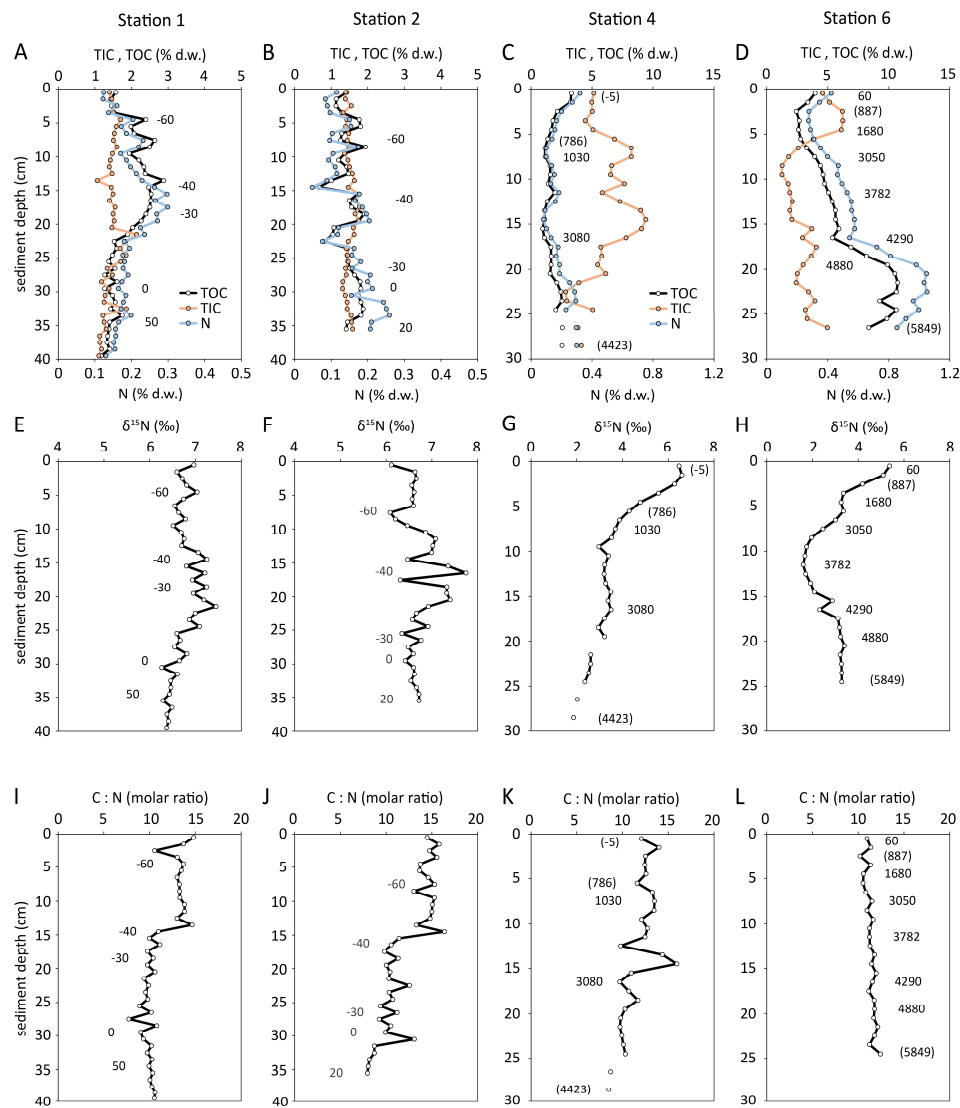


atmospheric N2 ( $\delta^{15}\text{N} = 0.0 \text{ ‰}$ ), while the distant stations were isotopically less enriched and were as light as 1.6 ‰. The nearshore sediment cores had higher concentration in organic matter than the more offshore cores.

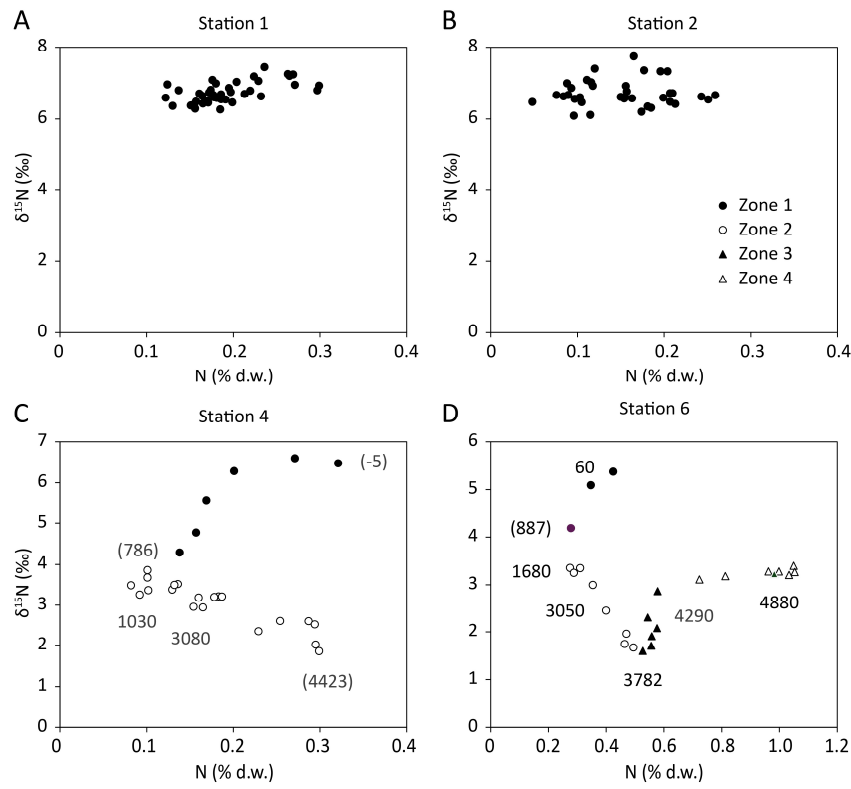
190 Sediment from stations 1 and 2 was distinct from stations 4 and 6 with respect to parameter values and their trends with sediment depth. In detail, sediment at station 1 had comparatively low contents of TOC (1.2 – 2.9 % d.w.), TIC (1.1 – 2.1 % d.w.), and N (0.12 – 0.30 % d.w.). While TOC and N had a maximum in 17 cm sediment depth, TIC had no discernible variation with sediment depth. The molar TOC / N ratio decreased from 15 at the sediment surface to 8 at 35 cm sediment depth. Sediment at station 2 was similarly low in TOC, TIC, and N and had only small variation with sediment depth. TOC  
195 contents were in the range of 0.7 to 1.9 % dry weight, the TIC contents in the range of 1.3 to 1.8 % dry weight, and N contents in the range of 0.05 to 0.26 % dry weight. The molar TOC / N ratio increased significantly from 8 at 35 cm sediment depth to 15 at the sediment surface, while no significant variation in  $\delta^{15}\text{N}$  values was observed (Fig. 3). The stations 4 and 6 on the continental slope were markedly different from stations 1 and 2. At station 6, small shell fragments of the bivalve *Modiolula phaseolina* were present in the upper 8 cm. Below 8 cm depth, bivalve shells of *Mytilus galloprovincialis* were found. At these  
200 stations, the organic carbon and nitrogen content decreases in the upper 3 to 7 cm of the cores (TOC 1.1 to 4.0 %; N 0.10 to 0.42 %, Fig. 3). At station 4, there is a slight increase in organic carbon (1.0 to 2.5 %) and nitrogen (0.10 to 0.30 %) content below 7 cm depth. The TOC and TN contents strongly increased with depth at station 6 (TOC: 2.7 to 9.2 %, N: 0.3 to 1.0 %). In contrast, the molar TOC / N ratios decreased with sediment depth at station 4 and slightly increased with depth at station 6 (Fig. 3 K, L).

205

Based on  $\delta^{15}\text{N}$  vs. N content plots, we identified 4 zones with distinct trends of N content and N isotopic signature. Zone 1 is the uppermost sediment layer where N content increased towards the sediment surface and N isotopes were most enriched (Fig. 4, filled circles). This was the only zone we could identify in the coastal stations 1 and 2. In the offshore stations 4 and  
210 6, Zone 2 further below has decreasing N content and increasing  $\delta^{15}\text{N}$  values (Fig. 4, open circles). Zone 3 was present only at station 6 and has constant N content but decreasing  $\delta^{15}\text{N}$  values, which were as low as 1.6 ‰ (Fig. 4, closed triangles). Zone 4 is characterised by decreasing N content but constant  $\delta^{15}\text{N}$  values of 3.3 ‰ (Fig. 4, open triangles). The measurements of sedimentary  $\delta^{15}\text{N}$  and N content from Zone 2 (see Fig. 4, open circles) from Stations 4 and 6 were further analysed for the apparent isotope enrichment factor ( $\epsilon$ ) by means of Rayleigh plots. The estimated values were  $\epsilon = -1.1 \pm 0.2 \text{ ‰}$  for Station 4,  
215 and  $\epsilon = 3.0 \pm 0.3 \text{ ‰}$  for Station 6, respectively (Fig. 5).



220 **Figure 3:** From Stations 1- 6, depth profiles of TIC (carbonate), TOC (organic sediment), total nitrogen (panels A - D), measured  
δ¹⁵N values of bulk sediment (panels E – H), and molar TOC / N ratio of organic sediment (panels I – L). Numbers refer to the  
sediment age BP (0 a BP = 1950 CE, negative age values are after 1950 CE, positive age values are before 1950 CE),  
based on <sup>210</sup>Pb (Stations 1, 2) and <sup>14</sup>C (Stations 4, 6). Numbers in parentheses were estimated by linear interpolation.  
<sup>210</sup>Pb data from Constantinescu et al. (2023).



225

Figure 4: Sedimentary  $\delta^{15}\text{N}$  vs. sedimentary nitrogen concentrations at Station 1 (A), Station 2 (B), Station 4 (C), and Station 6 (D). The different symbols indicate different process zones within the sediment column: Zone 1) filled circles indicate modern eutrophication, Zone 2) open circles indicate diagenetic enrichment, Zone 3) filled triangles indicate the gradual transition between two isotopically distinct nitrogen sources, and Zone 4) open triangles indicate unit II sapropel. Numbers refer to the  $^{14}\text{C}$ -based sediment age, numbers in parentheses were estimated by linear interpolation.

230

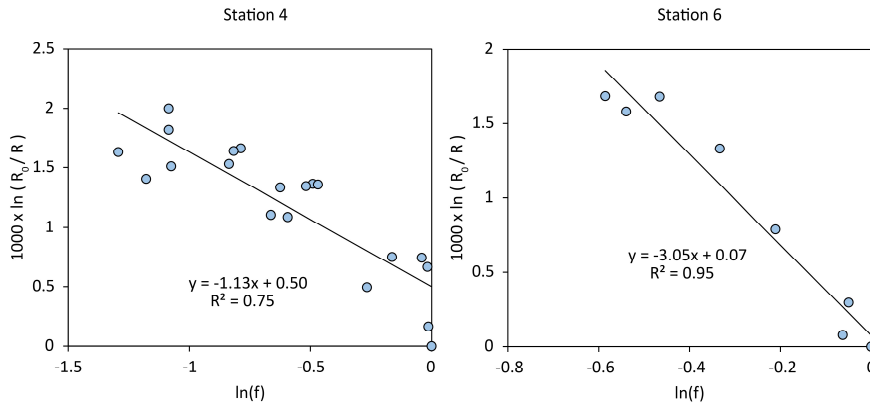


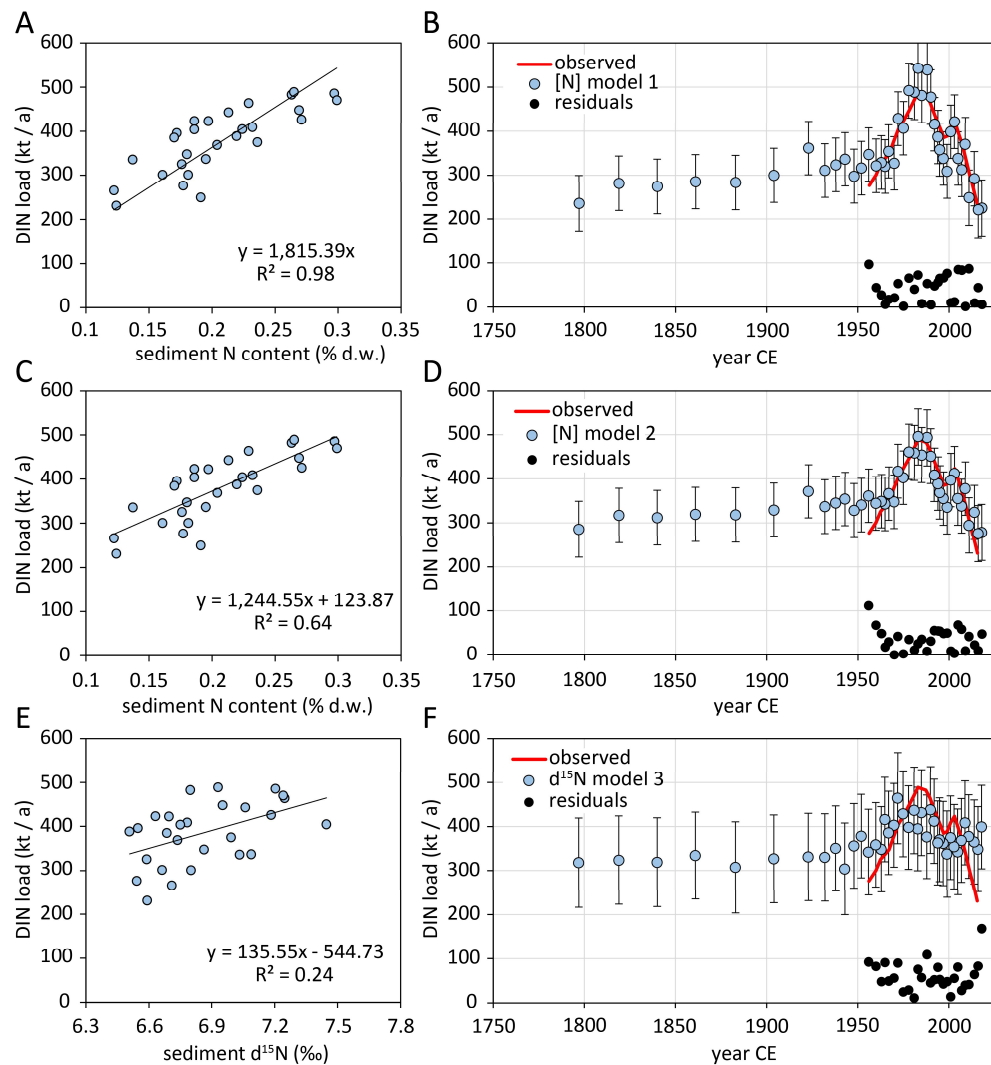
Figure 5: Rayleigh plots of  $\delta^{15}\text{N}$  vs. sedimentary N content of samples from Zone 2 of Stations 4 and 6 (see also Figure 4, open circles).

235

### 3.3 Correlation analyses

The correlation of Danube DIN load with sediment N content and  $\delta^{15}\text{N}$  values in the nearshore cores 1 and 2 was examined to develop a simple empirical model for reconstructing historical DIN loads for the period before measurements are available.

Using core 2, no meaningful correlation was found (not shown). Using core 1, the DIN load of Danube at Reni station (Kovacs 240 & Zavadsky, 2021) correlated significantly with the bulk N content (Pearson's  $R = 0.80$ ) and less significant with  $\delta^{15}\text{N}$  (Pearson's  $R = 0.35$ ). We derived two linear models from the DIN load – sediment N content correlation: Model 1 without y-intercept and Model 2 with y intercept. From the DIN load –  $\delta^{15}\text{N}$  correlation, we derived model 3. The N content-based Models 1 and 2 reconstruct the observed DIN loads of the 1955 – 2015 period reasonably well (Fig. 6 B, D). The  $\delta^{15}\text{N}$ -based Model 3 reconstructs the observed DIN load less accurately (Fig. 6 F). For the period 1800 – 1950, all three models 245 reconstructed that the Danube DIN load was 236 to 318 kt / yr in 1800 CE and increased gradually with 0.2 to 0.5 kt / yr<sup>2</sup>.



250 **Figure 6:** Linear correlations of Danube DIN loads with sediment N content (A, C) and sediment  $\delta^{15}\text{N}$  values (D), and reconstructed DIN loads based on these correlations (B, D, F). Error bars indicate prediction intervals with 90 % confidence. Red plots indicate DIN observation data for 1955 – 2015, data from Kovacs & Zavadsky (2021).



## 4 Discussion

### 4.1 Sedimentary signatures of major events in the Black Sea

255 The Black Sea has experienced several major events in the past 10 ka, which imprinted their specific signatures into the sediment record of the deep basins. However, as the sediment cores in our study were retrieved from the shallow nearshore shelf and the upper shelf slope, we discuss in the following the extend of the influence of basin-wide events on the nearshore sediment records. Since we sampled the most offshore and oldest sediment at station 6, we start with this sediment record.

260 At 5.8 ka BP, which is the age of the oldest sediment we have analysed at station 6, the Black Sea was influenced by Atlantic climate, which led to high freshwater discharge, a strong thermohaline stratification, and a shallow chemocline. The reconstructed  $\delta^{15}\text{N}$  value of phytoplankton during this period was in the range of 1.4 to 4.4 ‰ (Fulton et al. 2012). The Unit II b sapropel was deposited in the Black Sea basins during this phase, and we found similarly high TOC values in Core 6 and a matching  $\delta^{15}\text{N}$  value of 3.3 ‰ in sediment of this age (Fig. 3). We thus conclude that the N /  $\delta^{15}\text{N}$  trend of Zone 4 (Fig. 4, open 265 triangles) is equivalent with sediment unit II b.

The Atlantic phase lasted until approx. 5.1 ka BP, when the climate became colder and dryer. This sub- boreal climate resulted in substantially reduced riverine input, a weaker salinity gradient and thus a deeper circulation, which enhanced the pelagic ventilation. The concomitant upwelling of N- deficient and P- enriched water reduced the N : P ratio in the euphotic zone to 270 3.5 – 6, and the reconstructed  $\delta^{15}\text{N}$  value of phytoplankton during this period was in the range of 0.3 to 2.1 ‰ (Fulton et al. 2012). Although the basin-wide influx of riverine nutrients was reduced during this period, we found the highest rates of mass accumulation and carbon accumulation at this time (4.3 ka BP to 3.8 ka BP), and we conclude that the N /  $\delta^{15}\text{N}$  trend of Zone 3 (Fig. 4, closed triangles) is equivalent with sediment unit II a. The deeper ventilation of the pelagic resulted eventually in the oxygenation of the bottom water on the shelf and thus enabled enhanced diagenesis in the water column and of the upper 275 sediment layer. The result is advanced remineralisation of the sedimented organic matter with the corresponding N /  $\delta^{15}\text{N}$  trend of Zone 2 in cores 4 and 6 (Fig. 4, open circles). Cutmore et al. (2024) have not detected the proxy for H<sub>2</sub>S in the photic zone during this period (3.9 – 2.7 ka BP), which agrees with the time frame of Zone 2 in our samples. However, it seems that bottom water oxygenation happened at approx. 4.4 ka BP in the shallower station 4 (62 m) and thus significantly earlier than at the deeper station 6 (80 m) at which marked remineralization did not occurred before 3.8 ka BP. The differences in the onset of 280 remineralisation on the shelf could indicate the rate at which the oxycline descended. The deposition of coccoliths started during in this period (Hay et al. 1991, Coolen 2011), which is marked by and we find a substantial increase of carbonate content in sediment at from stations 4 and 6 from 3.0 to 2.5 ka BP onwards until approx. 0.8 ka BP (Fig. 3).

Around 2.1 ka BP, the sub-boreal climate gradually shifted to the current subatlantic climate with a trend towards warmer and 285 wetter climate and increased riverine influence (Fulton et al. 2012). The youngest major event reflected in core 6 is the massive



eutrophication during the ‘Green Revolution’ starting in the 1960s with intensive discharge of nutrients, which in turn resulted in enhanced primary production, enhanced oxygen consumption in deeper water layers, and thus a shallower oxycline. The increased deposition of organic matter with isotopically enriched nitrogen is evident in all cores and is described as Zone 1 (Fig. 4, closed circles).

290

In summary, the sediment cores of this study reflect all major events in the Black Sea of the past 6.000 years. Although we sampled sediment cores very close to the Danube Delta, we are confident that these sediments recorded signals from the Danube Plume and from the Black Sea, and that we can draw relevant conclusions from our results. In line with results of Fulton et al. (2012), our sedimentary analysis confirms that nitrogen cycling in the Black Sea was controlled by basin-wide processes, with its isotopic signatures spread throughout the Black Sea. Station 6 is influenced by the basin-wide Rim Current (Fig. 1), and the  $\delta^{15}\text{N}$  profile is similar to the 0-2 ka BP of the  $\delta^{15}\text{N}$  profile in Figure 4 in Fulton et al. (2012). We conclude that this core’s N-profile is rather determined by basin-wide processes. In contrast, the N distribution in cores 1 and 2 are more driven by the discharge of freshwater and nutrients from River Danube.

295

### 300 4.2 Nitrogen sources to the Northwestern Shelf

During the Atlantic climate phase between 6.9 to 5.1 ka BP, riverine discharge of freshwater was high, which led to a strong thermohaline stratification, low ventilation of the pelagic, and a shallow chemocline. The presence of isorenieratene in the sediment is interpreted as an indicator that the chemocline was so shallow that hydrogen sulphide ascended into the photic zone (Cutmore et al., 2024), and these euxinic conditions would have substantially constrained the degradation of sinking particles in the water column and in the sediment once they have been deposited. As a result, current isotopic values of sediment from this period are probably close to the original isotopic signature. With respect to nitrogen, we have measured a  $\delta^{15}\text{N}$  value of 3.3 ‰ in this sediment layer, which is consistent with riverine N from a pristine catchment with no anthropogenic land use (Johannsen et al. 2008, Bratek et al. 2020). And since freshwater discharge was high during the Atlantic climate phase, riverine N from Danube and adjacent rivers appears as the dominant N source to the NW shelf.

305

From 5.1 ka BP on, the climate changed into a subboreal phase with colder and dryer climate, less freshwater discharge, which resulted in less stratification and intensified ventilation of the pelagic (Fuller et al., 2012). This conclusion is supported by the absence of isorenieratene, in the 3.9 – 2.7 ka BP sediment layer, which indicates that the chemocline was much deeper during this period (Cutmore et al. 2024). The intensified and deeper mixing of the pelagic would not only mix oxygen downwards but would also enable the upward transport of nitrogen depleted and phosphate enriched deep water into the epipelagic. In combination with reduced discharge of riverine N, the upwelling would result in low N:P ratios and thereby set the stage for N-fixation. N-fixation has a strong negative isotopic effect and results in plankton matter with a comparatively low  $\delta^{15}\text{N}$  value in the range of approximately -2 to 1 ‰ (Minagawa & Wada 1986). In sediment from the period in which deep circulation



should have favoured N-fixation, we indeed observed a bulk sediment  $\delta^{15}\text{N}$  value as low as 1.6 ‰ at the most offshore station  
320 6 and found a similarly low  $\delta^{15}\text{N}$  value of 1.9 ‰ in station 4 sediment (Fig. 3, open circles). We thus conclude that the N  
source gradually shifted from riverine N to N-fixation in the 4.5 – 3.8 ka BP period.

At the time the isotopically most depleted nitrogen was sedimented, approximately from 3.6 ka BP onwards, carbonate  
cocoliths from the haptophyte plankton algae *Gephyrocapsa huxleyi* (formerly *Emiliania huxleyi*) started to accumulate in  
325 the sediment as cocolith ooze of Unit I (Hay et al. 1991, Xu et al. 2001, Coolen 2011), which raises the question of whether  
this is a coincidence. Low N:P ratios which favour N-fixation also enable *G. huxleyi* to form blooms (Lessard et al. 2005).  
Additionally, the cocolithophorid haptophyte *Braarudosphaera bigelowii* was demonstrated to host endosymbiotic,  
unicellular UCYN-A like cyanobacteria, which can fixate nitrogen (Thompson et al. 2012, Mills et al. 2020), and thereby  
provides a possible causation for the simultaneous deposition of cocoliths and isotopically depleted nitrogen. Moreover,  
330 Cutmore et al. (2024) found pentose heterocyte glycolipid (HG) in Black Sea sediment where the organic matter with the  
lowest  $\delta^{15}\text{N}$  was deposited and interpret this as an indicator for the presence of marine nitrogen-fixing cyanobacteria in  
symbiosis with marine diatoms. Finally, Coolen et al. (2009) found a single phylotype to dominate the *G. huxleyi* record in the  
3.4 to 2.6 ka BP period, which was absent before and after. While it is possible that the co-occurrence of cocoliths and  
isotopically depleted N in the sediment record is a coincidence, the combined observations hint to the possibility that *G. huxleyi*  
335 may have contributed to N-fixation in the Black Sea.

The intensified and deeper circulation during the sub-boreal phase resulted in an intensified ventilation of the shelf, which  
gradually increased the exposure of shelf sediments to oxygen and thereby enabled enhanced remineralisation of deposited  
organic matter there. Since Möbius et al. (2010) demonstrated that early diagenesis can alter the isotopic signature and thus  
340 overprinted the depleted isotope signature of N-fixation, we examined our results from Zone 2 of cores 4 and 6, where N  
contents decreased towards the surface while  $\delta^{15}\text{N}$  values increased. In core 4, the apparent enrichment factor of  $\varepsilon = -1.1 \pm 0.2$   
‰ falls well within the range of published values (Möbius et al. 2010) which supports our conclusion that the increase in  $\delta^{15}\text{N}$   
values in core 4 is result of remineralisation and not an indication of changes in nitrogen sources. However, the apparent  
enrichment factor of Zone 2 of core 6 with  $\varepsilon = -3.0 \pm 0.3$  ‰ is implausibly high. But the high apparent value can be explained  
345 if we assume a combination of early diagenesis and a gradual shift from N fixation to isotopically more enriched riverine input  
by the recent sub-atlantic climate phase. In summary, the more coastal station 4 appears being supplied by a mix of N-fixation  
and riverine N discharge between 4.4 – 1.0 ka BP. The more offshore station 6 was initially supplied by isotopically depleted  
nitrogen from N-fixation circa 3.8 ka BP, which was gradually complemented by isotopically enriched nitrogen until 1.3 ka  
BP (Fig. 4), and we assume that the enriched N was discharged by Danube and adjacent rivers as their discharge gradually  
350 increased over the past 3 ka BP (Giosan et al. 2012).



In cores from stations 4 and 6, the trend of decreasing N content and increasing  $\delta^{15}\text{N}$  in Zone 2 stops circa 0.8 ka BP, and N content and  $\delta^{15}\text{N}$  values increased substantially in younger sediment layers (Fig. 3, closed circles), which indicates increased deposition of organic matter with significantly isotopically enriched nitrogen. This enriched nitrogen is present in all sampled cores, and a plausible source of sufficiently enriched  $^{15}\text{N}$  is riverine discharge of nitrogen from anthropogenic activities such as agriculture and urbanization (Johannsen et al. 2008, Bratek et al. 2020). The effect of eutrophication due to anthropogenic activities is especially obvious in cores 1 and 2, where the  $\delta^{15}\text{N}$  values increase from  $6.6 \pm 0.1 \text{ ‰}$  in the 50 – 0 a BP period to  $7.1 \pm 0.1 \text{ ‰}$  in core 1 and  $6.9 \pm 0.5 \text{ ‰}$  in core 2 during the peak eutrophication during the 1980- 1990 period (-30 to -40 a BP, see Fig. 3). When the nitrogen load of Danube significantly dropped after the 1990s (Kovacs & Zavadsky, 2021), the  $\delta^{15}\text{N}$  values decreased along with the riverine nitrogen load back towards values below 7 ‰. It is noteworthy that the transition to substantially enriched N apparently happened around  $830 \pm 50$  a BP in both cores 4 and 6, and thus much earlier than the industrialisation in the 20<sup>th</sup> century when usage of artificial fertiliser became common.

The apparently early onset of isotopically enriched nitrogen deposition could be an artifact of bioturbation in which benthic macrofauna mixes modern, enriched nitrogen from the sediment surface downwards and thus into older sediment layers. The sediment cores retrieved at stations 4 and 6 were populated by sessile tunicates and small bivalves (*Modiolula phaseolina*), which are not strong bioturbators and are unlikely to provide sufficient sediment mixing to transport anthropogenic  $^{15}\text{N}$  down to 7 cm sediment depth at station 4. Our measurements of particle-associated  $^{210}\text{Pb}$  further indicates that the mixed surface layer reaches down to 4 cm at maximum (Fig. 2), which is significantly above the deepest occurrence of enriched nitrogen at 7 cm depth (Fig. 3). The much deeper penetration of  $^{137}\text{Cs}$  does not contradict our interpretation as  $^{137}\text{Cs}$  can have a much higher mobility in marine sediment as  $^{210}\text{Pb}$  and has probably migrated into deeper sediment layers as described by Wang et al. 2022. Additionally, the carbonate content of Cores 4 and 6 decreased simultaneously with increased  $\delta^{15}\text{N}$ , which is not a plausible result of sediment mixing by bioturbation. Instead, the decreasing carbonate content in the modern surface layer might indicate a change in the nutrient regime with a reduction of coccolithophorid blooms in the coastal area. Fulton et al. (2012) consistently found a significant increase of sediment  $\delta^{15}\text{N}$  values in cores from the shelf and deep basins, which starts around 0.5 ka BP and supports our observation that the deposition of enriched nitrogen started much earlier than the industrialisation.

An alternative explanation for the early deposition of enriched nitrogen is intensified N discharge during the Medieval Warm Period (Mann et al. 2009), which was a local climate optimum in Europe between 1000 a BP and 700 a BP and led to a substantial population growth with expansion of agricultural land use and urbanization in Europe. Giosan et al. (2012) presented the reconstructed land cover usage of the Danube river catchment area in which the share of anthropogenic land use exceeded 40 % at around 800 a BP and increased steeply afterwards. These 40 % of land use and the concomitant deforestation in a catchment area typically result in  $\delta^{15}\text{N}$  values of riverine nitrate of approximately 6 ‰ (Bratke et al. 2020), which is discharged into the Black Sea (Johannsen et al. 2008, Bratke et al. 2020) to be eventually deposited to the sea floor. The



hypothetical  $\delta^{15}\text{N}$  value of approximately 6 ‰ corresponds well with our observations in the sediment layer of that age (Fig. 3).

The pre-industrial eutrophication of the Danube River is further supported by our reconstruction of Danube DIN loads for the 390 19<sup>th</sup> century (Fig. 6). The modelled DIN loads based on correlations of observed DIN load and sedimentary bulk nitrogen content suggest that the Danube DIN load was in the range of 236 to 286 kt/a in 1800 CE, which is in the range of the current load (Kovacs & Zavadsky, 2021). Although the river DIN load with shelf sediment  $\delta^{15}\text{N}$  values were substantially less correlated than with shelf sediment bulk N content, the reconstructed DIN load based on  $\delta^{15}\text{N}$  is similar to the N content-based results. Additionally, the average slope of the Danube River DIN load trend in 1800 – 1950 of  $0.35 \pm 0.16 \text{ kt / yr}^2$  can be 395 linearly extrapolated approximately 800 years backwards until the modelled Danube River DIN load approaches zero. Although this extrapolation reaches very far into the past with respect to the relatively short period of underlying observation data and is thus a coarse estimate with a substantial amount of uncertainty, our model results are in line with an early onset of anthropogenic eutrophication of Danube. Our approach to reconstruct historical Danube River DIN loads relies on the 400 assumption that quantity and isotopic composition of Danube River DIN translates linearly to Black Sea sedimentary N content or bulk  $\delta^{15}\text{N}$  values, although the dissolved N is assimilated into phytoplankton, transported, deposited in the delta, and partially degraded by early diagenesis. The approach appears valid for the 1955 – 2015 period, and we are not aware of conflicting results to challenge our approximations of historic Danube DIN loads. The results of the offshore stations 4 and 6, which go 405 far back into the past, and the coastal station 1, which recorded the N deposition of the last 200 years in more detail, give a coherent picture of the steadily increasing eutrophication of the Danube for at least 800 years, which has only decreased again in the last 30 years. The sediment record of Station 2 is not reflecting these processes in sufficient detail likely due to its location on the active delta front slope (Fig. 1).

#### 4.3 Diagenetic overprint of the initial sediment record

We have already discussed above that euxinic conditions preserved the initial isotopic composition in the sapropel and that 410 ventilation of the bottom water resulted in a pronounced remineralisation of shelf sediment, which then led to changes in the isotopic composition of the remaining organic matter. Analogously, remineralisation apparently shifted the TOC / N ratio from 10 to 15 in the most exposed nearshore sediment (Fig. 3). The early diagenesis within the sediment could have additional consequences such as carbonate dissolution due to acidification of the porewater by  $\text{CO}_2$  production during remineralisation. The putative carbonate dissolution could explain the contradictory results that the presence of the plankton algae *Gephyrocapsa* 415 *huxleyi* in the Black Sea is proven by molecular evidence in the sediment (Coolen et al. 2009, Coolen 2011) since 7 ka BP, but the characteristic carbonate coccoliths are present in sediment cores only from 3.6 – 2.5 ka BP (Hay et al. 1991, Xu et al. 2001, Coolen 2011) onwards. The dissolution of old,  $^{14}\text{C}$ -depleted carbonate due to acidic porewater would produce correspondingly  $^{14}\text{C}$ -depleted DIC. Additionally, carbonate dissolution has a strong kinetic fractionation effect (Skidmore et al. 2004), which



420 depletes the produced DIC even further and may result in a complex pattern of age offsets (e.g. Barker et al. 2007). The isotopically depleted DIC ascends to the sediment surface by molecular diffusion and sediment compaction, where it is precipitated into carbonate shells of growing bivalves as demonstrated by Poirier et al. (2019) for benthic Foraminifers. Analogously, bivalves growing in  $^{14}\text{C}$ -depleted porewater would also appear older in radiocarbon dating than the surrounding organic sediment, and our radiocarbon dating results of shells at station 6 (Tab. 2). Ultimately, organic sediment and carbonate shells represent two different carbon pools, which are affected individually by early diagenesis. In our results, carbonate shells 425 appear systematically older than the surrounding organic sediment, while e.g. Hansen et al. (2022) report the opposite situation.

### Conclusions

430 We have sampled the sediment of the northwestern shelf of the Black Sea along a transect from the Danube Delta towards the shelf break, and analysed the content of TOC, TIC, total nitrogen and nitrogen stable isotope composition. Our results confirm previous findings that the contribution of riverine nitrogen and N-fixation fluctuated during the past 5,000 years and was 435 largely driven by climate changes. Our sediment samples from the western shelf enable us to estimate that the oxycline descended at the end of the Atlantic climate phase below 60 m water depth before 4.4 ka BP, and below 80 m at 3.7 ka BP. Due to the proximity of our sampling sites to the Danube Delta, which made the sediment record there susceptible to signals 440 from the Danube, we found that the deposition of isotopically enriched nitrogen started approximately 800 years ago. The deposition of substantial amounts of nitrogen from anthropogenic activities started surprisingly long before the industrialisation, which is believed to have started eutrophication in the 20<sup>th</sup> century. Our reconstructed DIN loads suggest that Danube was already eutrophicated at 1800 CE at a similar level as present, and that DIN loads gradually increased throughout the 19<sup>th</sup> century until 1960 CE, when eutrophication steeply increased and peaked around 1990 CE. The substantial reduction in Danube River DIN loads since 1990 due to efficient nutrient reduction policies in the Danube River catchment is already reflected in the western Black Sea coastal sediment record.

### Acknowledgement

445 We wish to thank the captain and the crew of the RV Mare Nigrum. We are grateful to M. Ankele, M. Metzke and N. Lahajnar for analytical work. We further thank L. Hoffman for the taxonomic identification of bivalve shells. This study was supported by the project ReCoReD (Reconstructing the Changing Impact of the Danube on the Black Sea and Coastal Region) funded by TNA FP7 EuroFleets 2, and by the DOORS project (European Commission, Grant 101000518). The International Atomic Energy Agency is grateful to the Government of the Principality of Monaco for the support provided to its IAEA Marine Environment Laboratories.



450 **References**

Anderson C, Cabana G. Does delta15N in river food webs reflect the intensity and origin of N loads from the watershed? *Sci Total Environ.* 2006 Aug 31;367(2-3):968-78. doi: 10.1016/j.scitotenv.2006.01.029. Epub 2006 Apr 17. PMID: 16616320.

455 Barker, S., W. Broecker, E. Clark, and I. Hajdas (2007), Radiocarbon age offsets of foraminifera resulting from differential dissolution and fragmentation within the sedimentary bioturbated zone, *Paleoceanography*, 22, PA2205, doi:[10.1029/2006PA001354](https://doi.org/10.1029/2006PA001354).

460 Bratek A., Kay-Christian Emeis, Tina Sanders, Scott D. Wankel, Ulrich Struck, Jürgen Möbius & Kirstin Dähnke (2020) Nitrate sources and the effect of land cover on the isotopic composition of nitrate in the catchment of the Rhône River, *Isotopes in Environmental and Health Studies*, 56:1, 14-35, DOI: 10.1080/10256016.2020.1723580

465 Bunzel, D., Milker, Y., Müller-Navarra, K., Arz, H.W., Friedrich, J., Lahajnar, N., Schmiedl, G., 2020. Integrated stratigraphy of foreland salt-marsh sediments of the south-eastern North Sea region. *Newsletters Stratigr.* 53, 415–442. <https://doi.org/10.1127/nos/2020/0540>

470 Constantinescu AM, Tyler AN, Stanica A, Spyros E, Hunter PD, Catianis I and Panin N (2023) A century of human interventions on sediment flux variations in the Danube-Black Sea transition zone. *Front. Mar. Sci.* 10:1068065. doi: 10.3389/fmars.2023.1068065

480 Coolen M. J. L.; James P. Saenz; Liviu Giosan; Nan Y. Trowbridge; Petko Dimitrov; Dimitar Dimitrov; Timothy I. Eglinton. (2009). *DNA and lipid molecular stratigraphic records of haptophyte succession in the Black Sea during the Holocene* , 284(3-4), 0–621. doi:10.1016/j.epsl.2009.05.029

475 Coolen M. J. L.. (2011). *7000 Years of *Emiliania huxleyi* Viruses in the Black Sea*. *Science*, 333(6041), 451–452. doi:10.1126/science.1200072

480 Cutmore, A., Bale, N., Hennekam, R., Yang, B., Rush, D., Reichart, G.-J., Hopmans, E. C., and Schouten, S.: Impact of deoxygenation and hydrological changes on the Black Sea nitrogen cycle during the Last Deglaciation and Holocene, *Clim. Past Discuss.* [preprint], <https://doi.org/10.5194/cp-2024-59>, in review, 2024.

Dähnke, K., A. Serna, T. Blanz, and K.-C. Emeis. 2008. Sub-recent nitrogen-isotope trends in sediments from Skagerrak (North Sea) and Kattegat: Changes in N-budgets and N-sources? *Marine Geology* 253: 92-98.



485 Fuchsman, C. A., Murray, J. W., & Konovalov, S. K. (2008). Concentration and natural stable isotope profiles of nitrogen species in the Black Sea. *Marine Chemistry*, 111(1), 90-105. <https://doi.org/https://doi.org/10.1016/j.marchem.2008.04.009>

Fulton J. M., M. A. Arthur, and K. H. Freeman (2012), Black Sea nitrogen cycling and the preservation of phytoplankton  $\delta^{15}\text{N}$  signals during the Holocene, *Global Biogeochem. Cycles*, 26, GB2030, doi:[10.1029/2011GB004196](https://doi.org/10.1029/2011GB004196).

490 Giosan, L., Coolen, M., Kaplan, J. *et al.* Early Anthropogenic Transformation of the Danube-Black Sea System. *Sci Rep* 2, 582 (2012). <https://doi.org/10.1038/srep00582>

495 Hansen, Katrine; Giraudeau, Jacques; Limoges, Audrey; Massé, Guillaume; Rudra, Arka; Wacker, L.; Sanei, Hamed; Pearce, Christof; Seidenkrantz, Marit-Solveig. (2021). Characterization of organic matter in marine sediments to estimate age offset of bulk radiocarbon dating. *Quaternary Geochronology*. 67. 101242. 10.1016/j.quageo.2021.101242.

500 Hay, Bernward J.; Arthur, Michael A.; Dean, Walter E.; Neff, Eric D.; Honjo, Susumu . (1991). *Sediment deposition in the Late Holocene abyssal Black Sea with climatic and chronological implications. Deep Sea Research Part A. Oceanographic Research Papers*, 38(), S1211–S1235. doi:10.1016/S0198-0149(10)80031-7

Johannsen A.; Kirstin Dähnke; Kay Emeis. (2008). *Isotopic composition of nitrate in five German rivers discharging into the North Sea* . 39(12), 0–1689. doi:10.1016/j.orggeochem.2008.03.004

505 Kaplan, J. O., Krumhardt, K. M. & Zimmermann, N. The prehistoric and preindustrial deforestation of Europe. *Quaternary Science Reviews* 28, 3016–3034 (2009).

510 Kovacs, A., & Zavadsky, I. (2021). Success and sustainability of nutrient pollution reduction in the Danube River Basin: recovery and future protection of the Black Sea Northwest shelf. *Water International*, 46(2), 176–194. <https://doi.org/10.1080/02508060.2021.1891703>

Lessard, Evelyn & Merico, Agostino & Tyrrell, Toby. (2005). Nitrate: Phosphate Ratios and *Emiliania huxleyi* Blooms. *Limnology and Oceanography*. 50. 1020-1024. 10.4319/lo.2005.50.3.1020.

515 Mann M. E. *et al.* Global Signatures and Dynamical Origins of the Little Ice Age and Medieval Climate Anomaly. *Science* 326,1256-1260(2009). DOI:[10.1126/science.1177303](https://doi.org/10.1126/science.1177303)



Maselli, V., Trincardi, F. Man made deltas. *Sci Rep* **3**, 1926 (2013). <https://doi.org/10.1038/srep01926>

Mills M.M., Turk-Kubo, K.A., van Dijken, G.L. *et al.* Unusual marine cyanobacteria/haptophyte symbiosis relies on N<sub>2</sub>

520 fixation even in N-rich environments. *ISME J* **14**, 2395–2406 (2020). <https://doi.org/10.1038/s41396-020-0691-6>

Minagawa, M. and Wada, E.: Nitrogen Isotope Ratios of Red Tide Organisms in the East-China-Sea – a Characterization of Biological Nitrogen-Fixation, *Mar. Chem.*, **19**, 245–259, 1986.

525 Möbius, J., Lahajnar, N., and Emeis, K.-C.: Diagenetic control of nitrogen isotope ratios in Holocene sapropels and recent sediments from the Eastern Mediterranean Sea, *Biogeosciences*, **7**, 3901–3914, <https://doi.org/10.5194/bg-7-3901-2010>, 2010.

Möbius, J., and K. Dähnke. 2015. Nitrate drawdown and its unexpected isotope effect in the Danube estuarine transition zone. *Limnology and Oceanography* **60**: 1008-1019.

530 Oguz, Temel & Tuğrul, Süleyman & Kideys, A. & Ediger, Vedat & Kubilay, Nilgun. (2005). Physical and biogeochemical characteristics of the Black Sea. *The Sea*. **14**. 1331-1369.

535 Oguz, T., Dippner, J. W., & Kaymaz, Z. (2006). Climatic regulation of the Black Sea hydro-meteorological and ecological properties at interannual-to-decadal time scales. *Journal of Marine Systems*, **60**(3-4), 235-254

Panin Nicolae, Laura Tiron Duțu and Florin Duțu, “The Danube Delta”, *Méditerranée*, **126** | 2016, 37-54. DOI: <https://doi.org/10.4000/mediterranee.8186>

540 Poirier, Clément; Baumann, Juliette; Chaumillon, Eric. (2019). Hypothetical influence of bacterial communities on the transfer of 14C-depleted carbon to infaunal Foraminifera: implications for radiocarbon dating in coastal environments. *Radiocarbon*. [10.1017/RDC.2019.7](https://doi.org/10.1017/RDC.2019.7).

545 Serna, A. and others 2010. History of anthropogenic nitrogen input to the German Bight/SE North Sea as reflected by nitrogen isotopes in surface sediments, sediment cores and hindcast models. *Continental Shelf Research* **30**: 1626-1638.

Skidmore M.; Martin Sharp; Martyn Tranter. (2004). *Kinetic isotopic fractionation during carbonate dissolution in laboratory experiments: Implications for detection of microbial CO<sub>2</sub> signatures using  $\delta^{13}\text{C-DIC}$* . **68**(21), 0-4317. doi:10.1016/j.gca.2003.09.024

550



Thompson A. W. *et al.*, Unicellular Cyanobacterium Symbiotic with a Single-Celled Eukaryotic Alga. *Science* **337**, 1546-1550(2012).DOI:10.1126/science.1222700

Wang J.L., M. Baskaran, N. Cukrov, J. Du (2022): Geochemical mobility of  $^{137}\text{Cs}$  in marine environments based on laboratory  
555 and field studies *Chem. Geol.*, 614, Article 121179

Xu L.; C.M. Reddy; J.W. Farrington; G.S. Frysinger; R.B. Gaines; C.G. Johnson; R.K. Nelson; T.I. Eglinton. (2001).  
*Identification of a novel alkenone in Black Sea sediments.* , 32(5), 0–645. doi:10.1016/s0146-6380(01)00019-5

560